

# Quantum evolution in the stroboscopic limit of repeated measurements

I. A. Luchnikov<sup>1</sup> and S. N. Filippov<sup>1,2</sup>

<sup>1</sup>*Moscow Institute of Physics and Technology, Institutskii Per. 9, Dolgoprudny, Moscow Region 141700, Russia*

<sup>2</sup>*Institute of Physics and Technology, Russian Academy of Sciences, Nakhimovskii Pr. 34, Moscow 117218, Russia*

We consider a quantum system dynamics caused by successive selective and non-selective measurements of the probe coupled to the system. For the finite measurement rate  $\tau^{-1}$  and the system-probe interaction strength  $\gamma$  we derive analytical evolution equations in the stroboscopic limit  $\tau \rightarrow 0$  and  $\gamma^2\tau = \text{const}$ , which can be considered as a deviation from the Zeno subspace dynamics on a longer timescale  $T \sim (\gamma^2\tau)^{-1} \gg \gamma^{-1}$ . Non-linear quantum dynamics is analyzed for selective stroboscopic projective measurements of an arbitrary rank. Non-selective measurements are shown to induce the semigroup dynamics of the system-probe aggregate. Both non-linear and decoherent effects become significant at the timescale  $T \sim (\gamma^2\tau)^{-1}$ , which is illustrated by a number of examples.

PACS numbers: 03.65.Xp, 03.65.Yz, 03.65.Ta

## I. INTRODUCTION

Measurements naturally provide some information about the system involved. In quantum physics, no information can be gained without disturbance of the system [1, 2]. The ultimate form of such a disturbance takes place in projective measurements, when the observation of a particular outcome  $i$  leads the system into the state  $|\psi_i\rangle$  (conditional state preparation). The mathematical form of the noise and disturbance relation has been recently found for general fuzzy observables [3]. The effect of system disturbance becomes more visible in sequential and repeated measurements.

By repeated measurements we mean successive measurements of the same quantum observable. For instance, a high repetition rate of the same projective measurement results in the quantum Zeno effect [4], in which the system state dynamics is frozen. Non-projective repeated measurements at finite frequency may also lead to a perfect freezing [5]. However, the accelerated decay is more ubiquitous in the case of a slow repetition rate of measurements (anti-Zeno effect) [6–8]. Since the conditional output state is non-linearly related with the input density operator, other non-trivial dynamics is possible including the emerging chaotic behavior [9, 10]. Repetitive measurements enable maintenance of quantum coherence in the presence of noise [11] or acceleration of decoherence [12]. Repeated selective measurements are applicable in ground state cooling [13]. Repetition of non-selective measurements at particular time moments allows controlling the probability of transitions between qubit levels [14].

By sequential measurements we mean successive measurements of different non-commuting quantum observables. Statistics of general sequential measurements may exhibit the properties of undecidability [15], universality with respect to the construction of a joint observable [16], and informational completeness for state tomography [17, 18]. Moreover, sequential measurements find applications in estimation of quantum system parameters [19], process tomography [20], one-way quantum computing [21], channel decoding [22], and detection [23] and generation [24] of non-classical correlations.

Periodic interventions in the quantum system evolution via unsharp measurements are analyzed in a series of pa-

pers [25–29]. In Ref. [25], restricted path integrals are used in the phenomenological treatment, which is equivalent to the introduction of non-Hermitian Hamiltonians. A particular physical realization of continuous measurements is considered in Ref. [26]. In Refs. [27, 28], two-outcome measurements of a qubit system are considered and the difference equations on the density operator are obtained by approximating the binomial distribution of outcomes by the Gaussian form. In Ref. [29], indirect measurements of a decaying system are realized via auxiliary states, with such coupling-based measurements increasing the decay rate.

In present paper, we develop the ideas of indirect measurements by introducing a probe, which interacts with the system and is periodically measured in equal time intervals  $\tau$ . The primary goal is to analyze the system dynamics caused by repeated measurements. The system-probe interaction Hamiltonian is arbitrary, with  $\gamma$  being the characteristic coupling strength. Our aim is to study the measurement-induced system dynamics at a timescale  $T \sim (\gamma^2\tau)^{-1}$  in contrast to the interaction timescale  $T_{\text{int}} \sim \gamma^{-1}$ . We show that in the *stroboscopic limit*  $\tau \rightarrow 0$ ,  $\gamma^2\tau = \text{const}$ , the resulting evolution allows an analytical solution for both selective and non-selective measurements. The stroboscopic limit implies  $\gamma\tau \ll 1$ , so the derived analytical solutions are valid at time  $T \gg T_{\text{int}}$  and can be interpreted as deviations from the Zeno dynamics at longer times. Note that we consider stroboscopic dynamics, which differs from so-called stroboscopic non-demolishing measurements of periodic quantities [30–33]. Conceptually, our approach is similar to that in Ref. [34], where the coupling dynamics is intervened by resets of the probe state or by renewal of the environment (cf. the collision model [35, 36]). However, the non-selective measurements cannot be reduced to resets, which differs in our model from those studied previously. Interestingly, the stroboscopic condition  $\gamma^2\tau = \text{const}$  resembles the analogous condition in the stochastic limit for calculating dominating contributions of the open system dynamics at long times [37].

The paper is organized as follows. In Sec. II, we formulate the problem of quantum evolution due to indirect stroboscopic measurements. In Sec. II A, we show that frequent observations of the probe via selective rank-1 projective measurements ( $\gamma\tau \ll 1$ ) effectively freeze the

probe evolution (Zeno subspace effect [38]) but the system evolution is non-linear and can be described by the analytical effective Hamiltonian at a timescale  $T \sim (\gamma^2 \tau)^{-1}$ . The introduced stroboscopic limit differs from the conventional limit in Zeno subspace effect [38, 39] and describes longer times when non-unitary effects become significant. In Sec. II B, projective measurements of an arbitrary rank  $r$  are considered. Such measurements enable the probe to evolve non-trivially within the measurement-invariant subspace, which affects the system evolution too. In Sec. III, general non-selective measurements of the probe are considered and a semigroup property of the system-probe dynamics is derived. In Sec. IV, brief conclusions are outlined.

## II. DYNAMICS UNDER STROBOSCOPIC SELECTIVE MEASUREMENTS

Let  $\mathcal{H}_{\text{sys}}$  and  $\mathcal{H}_{\text{pr}}$  be the system and probe Hilbert spaces, respectively. For the sake of simplicity we assume that both  $\mathcal{H}_{\text{sys}}$  and  $\mathcal{H}_{\text{pr}}$  are finite dimensional. By  $\mathcal{B}(\mathcal{H}_{\text{sys}})$  and  $\mathcal{B}(\mathcal{H}_{\text{pr}})$  denote the linear spaces of operators acting on  $\mathcal{H}_{\text{sys}}$  and  $\mathcal{H}_{\text{pr}}$ , respectively. Any system-probe Hamiltonian  $H$  admits the resolution

$$H = \gamma \sum_j A_j \otimes B_j, \quad (1)$$

where the dimensionless operators  $A_j \in \mathcal{B}(\mathcal{H}_{\text{sys}})$  and  $B_j \in \mathcal{B}(\mathcal{H}_{\text{probe}})$  have operator norms  $\|A_j\|_\infty, \|B_j\|_\infty \leq 1$ , with  $\|A\|_\infty = \max_{\psi: \langle \psi | \psi \rangle = 1} \sqrt{\langle \psi | A^\dagger A | \psi \rangle}$ . The parameter  $\gamma$  defines a characteristic strength of the system-probe interaction. Hereafter we assume the Planck constant  $\hbar = 1$ , so energy has the dimension of frequency.

Let  $\varrho$  be the aggregate density operator on  $\mathcal{H}_{\text{sys}} \otimes \mathcal{H}_{\text{pr}}$ , which describes the system and probe altogether ( $\varrho^\dagger = \varrho \geq 0$ ,  $\text{tr}[\varrho] = 1$ ). Then the unitary evolution of duration  $t$  reads

$$\mathcal{U}_t[\varrho] = e^{-iHt} \varrho e^{iHt}. \quad (2)$$

The probe is being measured repeatedly after equal time intervals  $\tau$ , see Figs. 1 and 2. We will refer to such an interrupted dynamics as a *stroboscopic* evolution. Note that this concept differs from stroboscopic measurements discussed in [30–33]. By time  $t = T$  the number of performed measurements equals  $N = \lfloor T/\tau \rfloor$ . If all those measurements resulted in the outcomes  $i_1, \dots, i_N$  sequentially, then the system-probe transformation is described by the following trace-decreasing map:

$$\Phi_T = \mathcal{U}_{T-N\tau} \circ \mathcal{I}_{i_N} \circ \dots \circ \mathcal{U}_\tau \circ \mathcal{I}_{i_2} \circ \mathcal{U}_\tau \circ \mathcal{I}_{i_1}, \quad (3)$$

where  $\circ$  denotes concatenation of maps and  $\mathcal{I}_{i_n}$  is the instrument describing the system-probe transformation if the outcome  $i_n$  is observed. Namely, the instrument is a completely positive trace-decreasing map such that the conditional output state is

$$\varrho_i = \frac{\mathcal{I}_i[\varrho]}{\text{tr}[\mathcal{I}_i[\varrho]]}. \quad (4)$$

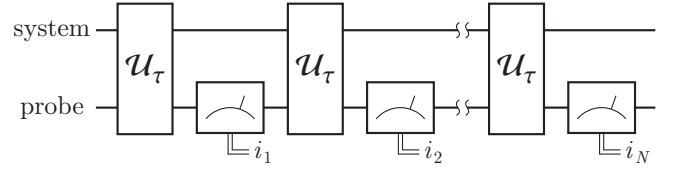


FIG. 1: Stroboscopic selective measurements of the probe result in a non-linear dynamics of the system.

Probability of realization of the map (3) for a given initial density operator  $\varrho$  equals  $p_\Phi = \text{tr}[\Phi_T[\varrho]]$ , where  $\text{tr}[\varrho] = 1$ .

Tracing out the probe, we get the system density operator evolution

$$\varrho_{\text{sys}}(T) = \text{tr}_{\text{pr}} \left\{ \frac{\Phi_T[\varrho(0)]}{\text{tr}[\Phi_T[\varrho(0)]]} \right\}. \quad (5)$$

We consider in detail the situation when the outcomes  $i_1, \dots, i_N = i$  are all coincident. Physically, the probability of such a sequence of outcomes is quite high if  $\gamma\tau \ll 1$  because this case corresponds to the quantum Zeno effect for the probe. This scheme resembles the repetition of pre- and post-selected measurements with identical pre- and post-selected states of the probe (state  $|i\rangle$ , see, e.g., the review [40]), however, no actual measurement of the system state is performed. Instead, the induced system dynamics is the primary goal of the study.

Observation of coincident outcomes  $i_k = i$ ,  $k = 1, \dots, N$  results in the following transformation:

$$\Phi_T = \mathcal{U}_{T-\lfloor T/\tau \rfloor \tau} \circ (\mathcal{U}_\tau \circ \mathcal{I}_i)^{\lfloor T/\tau \rfloor}. \quad (6)$$

For projective measurements the instrument  $\mathcal{I}_i$  takes the form of a trace-decreasing map with a single Kraus operator:

$$\mathcal{I}_i[\varrho] = C_i \varrho C_i, \quad C_i = I_{\text{sys}} \otimes P_i, \quad (7)$$

where  $P_i$  is a projector  $P_i = P_i^2 \in \mathcal{B}(\mathcal{H}_{\text{pr}})$ . We will refer to  $r = \text{rank} P_i$  as the rank of the measurement. If  $r = 1$ , then  $P_i = |\varphi\rangle\langle\varphi|$  and the observation of outcome  $i$  means that the probe state reduces to  $|\varphi\rangle\langle\varphi|$ . If  $r = \dim \mathcal{H}_{\text{pr}}$ , then such a measurement is completely uninformative as  $P_i = I_{\text{pr}}$ , the identity operator on the probe Hilbert space (no measurement in fact). The intermediate case  $1 < r < \dim \mathcal{H}_{\text{pr}}$  leaves some freedom for the probe evolution in the subspace  $\mathcal{H}_r = \text{supp} P_i$ , where  $\text{supp} P_i$  denotes the support of operator  $P_i$  (see Fig. 2).

It is natural to suppose that the initial state of the system and probe is factorized, i.e.  $\varrho(0) = \varrho_{\text{sys}}(0) \otimes \varrho_{\text{pr}}(0)$ , with  $\text{supp} \varrho_{\text{pr}}(0) \subseteq \text{supp} P_i$ , which is guaranteed by the first measurement. The system evolution

$$\varrho_{\text{sys}}(t) = \text{tr}_{\text{pr}} \left\{ \frac{\Phi_t[\varrho_{\text{sys}}(0) \otimes \varrho_{\text{pr}}(0)]}{\text{tr}[\Phi_t[\varrho_{\text{sys}}(0) \otimes \varrho_{\text{pr}}(0)]]} \right\} \quad (8)$$

is non-linear if  $H$  and  $C_i$  do not commute. Even though Eq. (8) is rather complicated, the approximate analytical solution can be found if the coupling strength  $\gamma$  and

the stroboscopic period  $\tau$  are appropriately related. In what follows, analytical solutions are derived and compared with the exact ones for various ranks  $r$  of the projector  $P_i$ .

### A. Analytical solution for rank-1 projectors

If  $r = 1$ , then  $C_i = I_{\text{sys}} \otimes |\varphi\rangle\langle\varphi|$  and  $\varrho_{\text{pr}}(0) = |\varphi\rangle\langle\varphi|$  for some fixed vector  $|\varphi\rangle \in \mathcal{H}_{\text{pr}}$ . We suppose the projective measurements are ideal and can be realized with a proper energy of the measuring device [41]. Rank-1 projectors are usually considered in the analysis of Zeno and anti-Zeno effects; however, our case crucially differs from those because the measurements are performed on the probe and not on the system itself. Though the probe dynamics is effectively frozen if  $\gamma\tau \rightarrow 0$ , the system continues evolving. If  $\gamma(T - \lfloor T/\tau \rfloor \tau) \ll 1$ , then the action of map  $\Phi_T$  can be approximated as follows:

$$\Phi_T[\varrho] \approx (\mathcal{U}_\tau \circ \mathcal{I}_i)^{T/\tau}[\varrho] = K \varrho K^\dagger, \quad (9)$$

where

$$K = (G(\gamma\tau))^{T/\tau}, \quad (10)$$

$$G(\gamma\tau) = \sum_{k=0}^{\infty} \sum_{j_1, \dots, j_k} \frac{(-i\gamma\tau)^k}{k!} A_{j_1} \cdots A_{j_k} \langle B_{j_1} \cdots B_{j_k} \rangle, \quad (11)$$

$$\langle B_{j_1} \cdots B_{j_k} \rangle = \langle \varphi | B_{j_1} \cdots B_{j_k} | \varphi \rangle.$$

If  $T/\tau$  is an integer, then Eq. (9) becomes exact. The approximate form of the Kraus operator  $K$  can be rewritten in the following form:

$$K = \exp \left\{ -iT \left[ \frac{i}{\tau} \ln G(\tau\gamma) \right] \right\}, \quad (12)$$

which can be simplified under the circumstances

$$\tau \rightarrow 0, \quad \gamma^2 \tau = \Omega = \text{const} \quad (13)$$

referred to as a *stroboscopic limit*.

The physical meaning of the stroboscopic limit (13) is that  $\gamma\tau \rightarrow 0$ , i.e. the probe dynamics is effectively frozen (the quantum Zeno effect) but the system dynamics is not frozen. The mathematical machinery is as follows. Changing the variables  $\gamma$  and  $\tau$  by  $\Omega = \gamma^2 \tau$  and  $\varkappa = \sqrt{\tau}$ , one can expand the logarithm in Eq. (12) in the vicinity of  $\varkappa = 0$ :

$$\ln G(\sqrt{\Omega} \varkappa) = -i\sqrt{\Omega} \varkappa \sum_j A_j \langle B_j \rangle - \frac{\Omega \varkappa^2}{2} \sum_{jk} A_j A_k \left( \langle B_j B_k \rangle - \langle B_j \rangle \langle B_k \rangle \right) + O(\varkappa^3). \quad (14)$$

Substituting Eq. (14) in Eq. (12) yields

$$K = e^{-iH_{\text{eff}} T}, \quad (15)$$

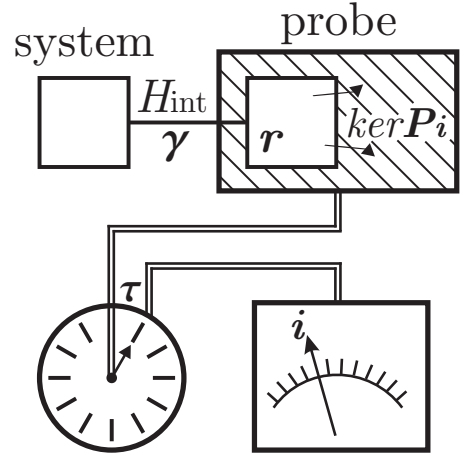


FIG. 2: Schematic of stroboscopic evolution. Probe is being measured at successive moments with equal time intervals  $\tau$  between them. Characteristic strength of the system-probe interaction is  $\gamma$ . Rank- $r$  measurements of the probe restrict the system-probe evolution to the subspace  $\mathcal{H}_{\text{sys}} \otimes \mathcal{H}_r$ , where  $\mathcal{H}_{\text{pr}} = \mathcal{H}_r \oplus \ker P_i$ .

where the effective Hamiltonian  $H_{\text{eff}}$  reads

$$H_{\text{eff}} = H_1 - iH_2 + O(\sqrt{\tau}), \quad (16)$$

$$H_1 = \gamma \sum_j A_j \langle B_j \rangle, \quad (17)$$

$$H_2 = \frac{\Omega}{2} \sum_{jk} A_j A_k (\langle B_j B_k \rangle - \langle B_j \rangle \langle B_k \rangle). \quad (18)$$

Both  $H_1$  and  $H_2$  are Hermitian and, besides,  $H_2 \geq 0$ . In fact, it is not hard to see that  $H_2 = \frac{\tau}{2} D_i^\dagger D_i$ , where  $D_i = (I - C_i) H I_{\text{sys}} \otimes |\varphi\rangle$ . The fact  $H_2 \geq 0$  implies the trace-decreasing property of the map (9). Note that  $H_2 \neq 0$  if and only if  $(I - C_i) H C_i \neq 0$ , i.e. the original Hamiltonian causes transitions between the sectors  $\text{supp} P_i$  and  $\ker P_i$ . The covariance matrix  $M_{jk} = \langle B_j B_k \rangle - \langle B_j \rangle \langle B_k \rangle$  quantifies the intensity of such transitions.

The normalized system state  $\varrho_{\text{sys}}(T)$  satisfies the non-linear equation

$$\frac{\partial \varrho_{\text{sys}}}{\partial T} = -i[H_1, \varrho_{\text{sys}}] - \{H_2, \varrho_{\text{sys}}\} + 2\text{tr}(H_2 \varrho_{\text{sys}}) \varrho_{\text{sys}}, \quad (19)$$

where  $\{\cdot, \cdot\}$  denotes the anticommutator. The purity parameter  $\text{tr}[\varrho_{\text{sys}}^2]$  evolves non-monotonically in general because the sign of derivative

$$\frac{\partial}{\partial T} \text{tr}[\varrho_{\text{sys}}^2] = 4(\text{tr}[\varrho_{\text{sys}}^2] \text{tr}[H_2 \varrho_{\text{sys}}] - \text{tr}[H_2 \varrho_{\text{sys}}^2]) \quad (20)$$

depends on  $H_2$  and  $\varrho_{\text{sys}}$ .

Suppose the initial state  $\varrho_{\text{sys}}(0)$  is pure. Then the approximate dynamics (19) preserves purity of the initial state and the evolution of system state vector  $|\psi\rangle$  satisfies

$$i \frac{\partial |\psi\rangle}{\partial T} = (H_1 - iH_2) |\psi\rangle + i \langle \psi | H_2 | \psi \rangle |\psi\rangle. \quad (21)$$

Analogous equations are used in stochastic interpretation of open quantum system dynamics [42]. If we recall the

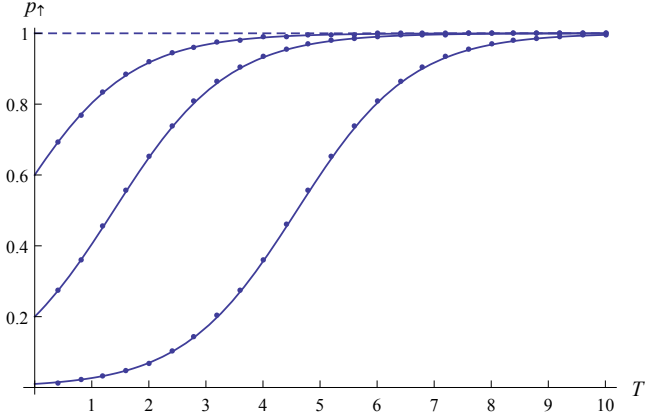


FIG. 3: Comparison of exact (dots) and analytical (solid line) expressions (24) for probability of finding the qubit system in the excited state at time  $T$  as a result of the stroboscopic evolution (8) and its description via the effective Hamiltonian (16) with  $\gamma = 5$ ,  $\tau = 0.04$ ,  $\Omega = 1$ , and the initial state of the system is  $|\psi(0)\rangle = \alpha|\uparrow\rangle + \beta|\downarrow\rangle$ , where  $|\alpha|^2 = 0.01$ ,  $|\beta|^2 = 0.99$  (bottom line),  $|\alpha|^2 = 0.2$ ,  $|\beta|^2 = 0.8$  (middle line), and  $|\alpha|^2 = 0.6$ ,  $|\beta|^2 = 0.4$  (top line). Dashed line corresponds to the evolution with initial state  $|\psi(0)\rangle = |\uparrow\rangle$ .

exact dynamics according to Eq. (8), then at each time  $t = n\tau$ ,  $n \in \mathbb{N}$ , the exact density operator  $\varrho_{\text{sys}}(n\tau)$  is also pure as a result of the measurement performed. In between, the exact density operator  $\varrho_{\text{sys}}(t)$  can become mixed but the less the product  $\gamma\tau$  the greater is the purity  $\text{tr}[\varrho_{\text{sys}}^2(t)]$ . In the stroboscopic limit (13), the exact dynamics (8) reduces to Eqs. (19)–(21).

Let us illustrate the developed theory for a physical system of two coupled qubits ( $\dim \mathcal{H}_{\text{sys}} = \dim \mathcal{H}_{\text{pr}} = 2$ ), one of which is being frequently measured with a finite rate  $\tau^{-1}$ .

**Example 1.** Let two qubits interact with Hamiltonian  $H = \gamma \text{SWAP} = \frac{\gamma}{2} \sum_{j=0}^3 \sigma_j \otimes \sigma_j$ , where  $\sigma_0 = I$  and  $(\sigma_1, \sigma_2, \sigma_3)$  is the conventional set of Pauli operators (Heisenberg Hamiltonian for spins). By  $U_\tau = e^{-iH\tau}$  denote the evolution operator for a period  $\tau$ . Suppose  $P_i = \varrho_{\text{pr}}(0) = |\uparrow\rangle\langle\uparrow|$ , where  $\sigma_3|\uparrow\rangle = |\uparrow\rangle$  and  $\sigma_3|\downarrow\rangle = -|\downarrow\rangle$ , i.e. one stroboscopically measures the particular spin projection of the probe qubit. Then

$$U_\tau |\psi\rangle \otimes |\uparrow\rangle = \cos \gamma\tau |\psi\rangle \otimes |\uparrow\rangle - i \sin \gamma\tau |\uparrow\rangle \otimes |\psi\rangle \quad (22)$$

and the Kraus operator for a period  $\tau$  reads  $K_\tau = (I_{\text{sys}} \otimes P_i)U_\tau = e^{-i\gamma\tau} |\uparrow\rangle\langle\uparrow| + \cos \gamma\tau |\downarrow\rangle\langle\downarrow|$ . Since  $(\cos \gamma\tau)^{T/\tau} \rightarrow \exp(-\frac{1}{2}\Omega T)$  in the stroboscopic limit (13),  $K = K_\tau^{T/\tau} = \exp(-iH_{\text{eff}}T)$ , where the effective system Hamiltonian reads

$$H_{\text{eff}} = \gamma |\uparrow\rangle\langle\uparrow| - i\frac{\Omega}{2} |\downarrow\rangle\langle\downarrow|. \quad (23)$$

Formula (16) gives the same result. Suppose the initial system state is  $|\psi(0)\rangle = \alpha|\uparrow\rangle + \beta|\downarrow\rangle$ ,  $|\alpha|^2 + |\beta|^2 = 1$ , then at time  $T = N\tau$  the probability to find the system in the state  $|\uparrow\rangle$  equals

$$p_\uparrow = \frac{|\alpha|^2}{|\alpha|^2 + (\cos \gamma\tau)^{2N} |\beta|^2} \approx \frac{|\alpha|^2}{|\alpha|^2 + e^{-\Omega T} |\beta|^2}, \quad (24)$$

where the left hand side of (24) is the exact expression and the right hand side of (24) is obtained via the effective Hamiltonian. Comparison of exact numerical and approximate analytical results is presented in Fig. 3.

The non-linear effects become relevant at time  $\sim \Omega^{-1}$  with the increase in the probability of error  $p_{\text{err}} = 1 - p_\Phi$ , which happens when the measurement outcome  $i_k \neq i$ . In the example above,  $p_{\text{err}} = |\beta|^2(1 - e^{-\Omega T})$ . Therefore, there is a trade-off between non-linearity and the probability of its physical observation.

## B. Analytical solution for rank- $r$ projectors

Let us now consider the case when  $P_i$  in formula (7) is a rank- $r$  projector. Physically it corresponds to a measurement of an incomplete set of variables. For instance, measurement of the square of the spin angular momentum,  $\mathbf{s}^2$ , and observation of the outcome  $s(s+1)$  does not specify the spin projection  $m = s, s-1, \dots, -s$ , i.e.  $r = 2s+1$ . Due to degeneracy of  $P_i$ , the probe is not frozen (in contrast to  $r = 1$ ), which is known as a Zeno subspace effect [38, 39]. The probe dynamics is restricted to the subspace  $\text{supp} P_i$  and the subspace  $\ker P_i$  is forbidden (see Fig. 2). Thus, the system-probe dynamics takes place in the space  $\mathcal{H}_{\text{sys}} \otimes \mathcal{H}_r$  and can be additionally simplified if the condition (13) is fulfilled.

Introduce the operators

$$G_j = P_i B_j P_i, \quad G_{jk} = P_i B_j B_k P_i, \quad (25)$$

which generalize Eq. (11). Restricting ourselves to the subspace  $\text{supp} C_i$ , we see that the operator  $C_i$  acts as the identity operator on all vectors  $|\xi\rangle \in \text{supp} C_i$ . In the domain  $\text{supp} C_i$  we have

$$\begin{aligned} & \ln \left[ C_i - i\gamma\tau \sum_j G_j - \frac{\gamma^2\tau^2}{2} \sum_{jk} G_{jk} + O((\gamma\tau)^3) \right] \\ &= -i\gamma\tau \sum_j G_j - \frac{\gamma^2\tau^2}{2} \sum_{jk} (G_{jk} - G_j G_k) + O((\gamma\tau)^3). \end{aligned}$$

Continuing the same line of reasoning as in Sec. II A, we obtain in the stroboscopic limit (13) that the system-probe density operator  $\varrho$  evolves in the subspace  $\text{supp} C_i$  according to the following equation:

$$\varrho(T) = \Phi_T[\varrho_{\text{sys}}(0) \otimes \varrho_{\text{pr}}(0)] \approx e^{-iH_{\text{eff}}T} \varrho_{\text{sys}}(0) \otimes \varrho_{\text{pr}}(0) e^{iH_{\text{eff}}^\dagger T}, \quad (26)$$

where the effective Hamiltonian  $H_{\text{eff}}$  reads

$$H_{\text{eff}} = H_1 - iH_2 + O(\sqrt{\tau}), \quad (27)$$

$$H_1 = \gamma \sum_j A_j \otimes G_j, \quad (28)$$

$$H_2 = \frac{\Omega}{2} \sum_{jk} A_j A_k \otimes (G_{jk} - G_j G_k). \quad (29)$$

By the same arguments, the term  $H_2 = \frac{\tau}{2} \text{tr}_{\text{pr}}[C_i H (I - C_i) H C_i] \geq 0$  is responsible for trace decreasing.

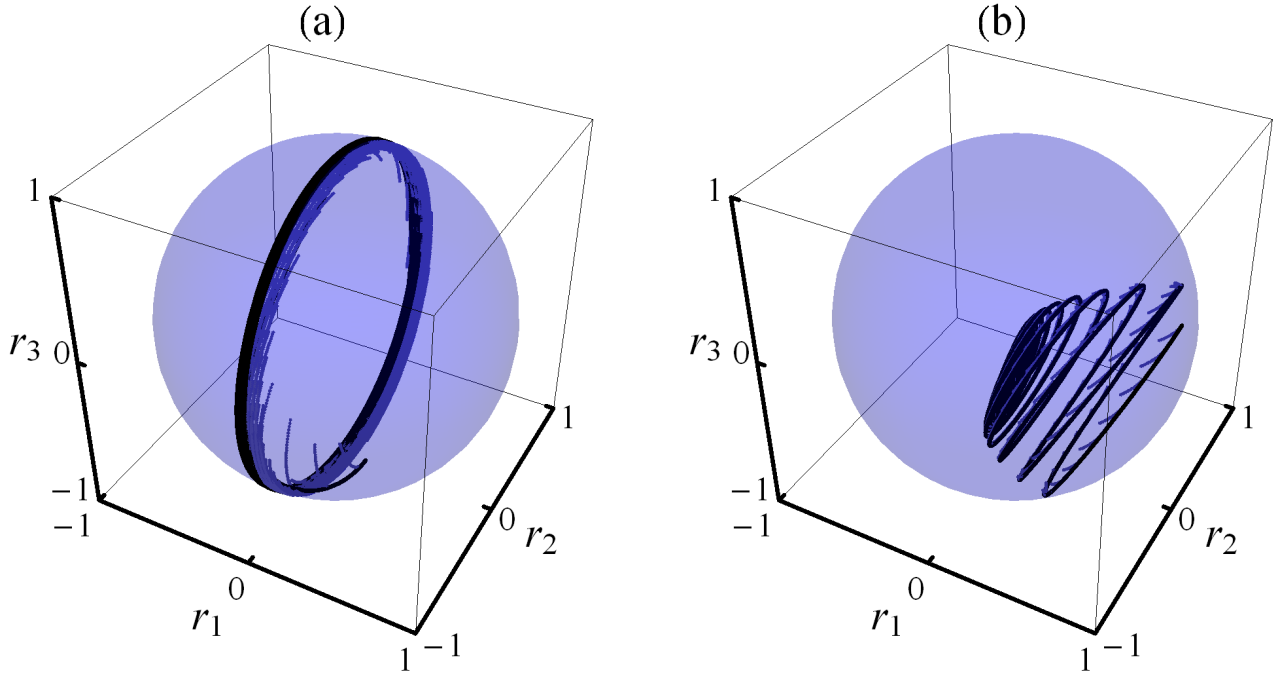


FIG. 4: Qubit evolution  $\varrho_{\text{sys}}(t) = \frac{1}{2}(I + \sum_{i=1}^3 r_i(t)\sigma_i)$  as a result of system-probe nonlinear stroboscopic dynamics. Discontinuous line depicts the exact evolution and emphasizes the stroboscopic character of measurements [formulas (6) and (8)]. Continuous black line is the analytical approximate solution. (a) Limit cycle in Example 2, (b) dynamics inside the Bloch ball in Example 3.

Despite the fact that the system-probe dynamics is governed by the effective Hamiltonian (27), the dynamics of system state  $\varrho_{\text{sys}}$  is not described by the effective Hamiltonian in general and must be obtained via tracing out the probe. Comparison of the exact system evolution [given by Eqs. (3) and (8)] and the approximate analytical system evolution [given by Eqs. (26) and (8)] is presented in the following examples.

**Example 2.** Consider three qubits (labelled  $a, b, c$ ), where qubit  $a$  is a system and two qubits  $b$  and  $c$  represent a probe. Let  $P_i = |S=0, M=0\rangle\langle S=0, M=0| + |S=1, M=0\rangle\langle S=1, M=0|$  be a projector onto subspace with zero total spin projection of the probe. In conventional notation  $P_i = |\uparrow_b\downarrow_c\rangle\langle\uparrow_b\downarrow_c| + |\downarrow_b\uparrow_c\rangle\langle\downarrow_b\uparrow_c|$ ,  $\text{rank} P_i = 2$ . Suppose the Heisenberg interaction Hamiltonian of three qubits in local external fields,  $H = \gamma(\vec{\sigma}^a\vec{\sigma}^b + \vec{\sigma}^b\vec{\sigma}^c + \vec{\sigma}^c\vec{\sigma}^a + \sigma_x^a + \sigma_y^b + \sigma_z^c)$ . Then stroboscopic measurements with  $\tau = 0.04$  and  $\gamma = 5$  satisfy  $\gamma\tau \ll 1$ , and the stroboscopic theory can be applied. Comparison of the exact and approximate dynamics of qubit  $a$  is depicted in Fig. 4(a). Dynamics represents a limit cycle, which manifests the non-linear character of evolution.

**Example 3.** In the above example of three qubits (labelled  $a, b, c$ ), change the projector  $P_i = |S=1, M=1\rangle\langle S=1, M=1| + |S=1, M=-1\rangle\langle S=1, M=-1| = |\uparrow_b\uparrow_c\rangle\langle\uparrow_b\uparrow_c| + |\downarrow_b\downarrow_c\rangle\langle\downarrow_b\downarrow_c|$  and consider Heisenberg interaction Hamiltonian of three qubits in a global external field,  $H = \gamma(\vec{\sigma}^a\vec{\sigma}^b + \vec{\sigma}^b\vec{\sigma}^c + \vec{\sigma}^c\vec{\sigma}^a + \sigma_z^a + \sigma_z^b + \sigma_z^c)$ . Stroboscopic measurements with  $\tau = 0.02$  and  $\gamma = 2\sqrt{2}$

satisfy  $\gamma\tau \ll 1$ , and one can use the approximate formula of the stroboscopic limit. Comparison of the exact and approximate dynamics of qubit  $a$  inside the Bloch ball is depicted in Fig. 4(b). The decrease of the system state purity can be attributed to the entanglement between the system and the probe. In fact, the map (26) is bipartite with respect to the system and the probe; entanglement preserving and entanglement annihilating properties of bipartite maps are characterized [43].

The above examples show that the analytical approximate results are in perfect agreement with the exact numerical ones.

### III. STROBOSCOPIC LIMIT FOR NON-SELECTIVE MEASUREMENTS

For the sake of generality we do not single out the system and the probe in the beginning of this section, so we deal with a general Hilbert space  $\mathcal{H}_{\text{sys+pr}}$ . Let us consider a non-selective projective measurement described by the trace-preserving completely positive map (measurement channel)

$$\Lambda[\varrho] = \sum_{i=1}^m C_i \varrho C_i, \quad (30)$$

where each operator  $C_i = C_i^2$  is a projector and  $m$  is a number of Kraus operators,  $\sum_{i=1}^m C_i = I$ . There is no restriction on the dimension of projectors, i.e.  $\dim \text{supp} C_i$



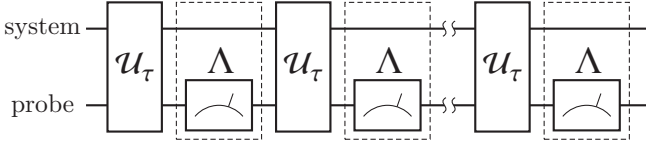


FIG. 5: Stroboscopic non-selective measurements. Though the unitary evolution is interrupted by measurements (30), the dynamics is not frozen in  $\text{supp}\Lambda$ .

is arbitrary, with  $\sum_{i=1}^m \dim \text{supp} C_i = \dim \mathcal{H}_{\text{sys+pr}}$ . Note that

$$\Lambda \circ \Lambda = \Lambda \quad (31)$$

since  $C_i C_j = \delta_{ij} C_j$ .

Suppose non-selective measurements (30) are performed successively after equal time intervals of duration  $\tau$ , with the intermediate unitary evolution being described by Eq. (2), see Fig. 5. Such a stroboscopic dynamics with non-selective measurements defines the dynamical map

$$\Phi_T = \mathcal{U}_{T-N\tau} \circ \Lambda \circ \dots \circ \Lambda \circ \mathcal{U}_\tau \circ \Lambda \circ \mathcal{U}_\tau, \quad (32)$$

which describes the exact evolution. It is natural to assume that the initial state  $\varrho(0)$  is an eigenstate of  $\Lambda$ , i.e.  $\Lambda[\varrho(0)] = \varrho(0)$ . If this is not the case, one can set  $t = 0$  at the moment of the first measurement.

At times  $T = n\tau$ ,  $n \in \mathbb{N}$ , the transformation  $\Phi_T$  maps any operator into  $\text{supp}\Lambda$ . For instance, the density matrix at such time moments has the form

$$\varrho(T) = \begin{pmatrix} \rho^{(1)}(T) & & & 0 \\ & \rho^{(2)}(T) & & \\ & & \ddots & \\ 0 & & & \rho^{(m)}(T) \end{pmatrix} \quad (33)$$

in the basis of eigenvectors of  $C_i$ , where  $\rho^{(i)}(T)$  is a restriction of the operator

$$\varrho^{(i)}(T) = C_i \varrho(T) C_i \quad (34)$$

to the subspace  $\text{supp} C_i$ . Eq. (34) would represent a conditional density operator if the outcome  $i$  was observed. In other words,  $\rho^{(i)}(T)$  is a non-zero minor of the matrix representation of  $\varrho^{(i)}(T)$  in the basis of eigenvectors of  $C_i$ .

In what follows we derive analytical equations for the approximate dynamics of  $\varrho(T)$  in  $\text{supp}\Lambda$  in the stroboscopic limit.

For the sake of generality we do not impose any restrictions on the Hamiltonian  $H$  except extracting its characteristic strength explicitly, i.e.  $H = \gamma h$ , where  $h$  is dimensionless and its operator norm  $\|h\|_\infty \leq 1$ . Then the unitary map  $\mathcal{U}_t = \exp(\gamma \mathcal{L}t)$ , where the generator  $\mathcal{L}$  reads

$$\mathcal{L}[\varrho] = -i[h, \varrho]. \quad (35)$$

Approximate formula for the dynamical map is

$$\Phi_T = \Lambda \circ \exp[\gamma \tau \mathcal{L}] \circ \Lambda \circ \dots \circ \Lambda \circ \exp[\gamma \tau \mathcal{L}] \circ \Lambda, \quad (36)$$

where we have taken into account that  $\Lambda[\varrho(0)] = \varrho(0)$ . Using the property (31), we get

$$\begin{aligned} \Phi_T &= [\Lambda \circ \exp(\gamma \tau \mathcal{L}) \circ \Lambda]^{T/\tau} = \left[ \sum_{k=0}^{\infty} \frac{(\gamma \tau)^k}{k!} \Lambda \circ \mathcal{L}^k \circ \Lambda \right]^{T/\tau} \\ &= \exp \left\{ T \left[ \frac{1}{\tau} \ln \left( \sum_{k=0}^{\infty} \frac{(\gamma \tau)^k}{k!} \Lambda \circ \mathcal{L}^k \circ \Lambda \right) \right] \right\}. \end{aligned} \quad (37)$$

Some algebra in the stroboscopic limit  $\gamma^2 \tau = \Omega$ ,  $\tau \rightarrow 0$  yields

$$\Phi_T = \exp(\mathcal{L}_{\text{eff}} T), \quad (38)$$

where the effective dynamical semigroup generator [44, 45] reads

$$\mathcal{L}_{\text{eff}} = \gamma \Lambda \circ \mathcal{L} \circ \Lambda + \frac{\Omega}{2} (\Lambda \circ \mathcal{L}^2 \circ \Lambda - \Lambda \circ \mathcal{L} \circ \Lambda \circ \mathcal{L} \circ \Lambda). \quad (39)$$

The fact that the measurement-induced dynamics reduces to a dynamical semigroup in the stroboscopic limit is in agreement with the earlier studies, where master equations were derived for calculation of the modified decay rates [6, 46].

To get the particular form of the generator (39) for the system-probe Hamiltonian  $H = \gamma h$ , we introduce auxiliary operators

$$h_{ij} = C_i h C_j, \quad (40)$$

whose physical meaning is the transition between measurement-invariant subspaces  $\text{supp} C_j$  and  $\text{supp} C_i$ . Note that  $h_{ij}$  denotes an operator not a matrix element. We substitute (35) into each term of (39) and expand

$$\Lambda \circ \mathcal{L} \circ \Lambda[\varrho] = -i \sum_i [h_{ii}, \varrho], \quad (41)$$

$$\Lambda \circ \mathcal{L} \circ \Lambda \circ \mathcal{L} \circ \Lambda[\varrho] = - \sum_i \{h_{ii}^2, \varrho\} - 2h_{ii} \varrho h_{ii}, \quad (42)$$

$$\Lambda \circ \mathcal{L}^2 \circ \Lambda[\varrho] = - \sum_{ij} \{h_{ji}^\dagger h_{ji}, \varrho\} - 2h_{ji} \varrho h_{ji}^\dagger \quad (43)$$

to get the final expression for the effective dynamical semigroup generator in the Lindblad form:

$$\mathcal{L}_{\text{eff}}[\varrho] = -i\gamma \sum_i [h_{ii}, \varrho] - \frac{\Omega}{2} \sum_{i \neq j} \left( \{h_{ji}^\dagger h_{ji}, \varrho\} - 2h_{ji} \varrho h_{ji}^\dagger \right). \quad (44)$$

One can see that the non-transition operators  $h_{ii}$  are responsible for the unitary evolution, whereas the transition operators  $h_{ij}$ ,  $i \neq j$  are exactly the Lindblad operators responsible for the dissipation and decoherence. Because  $h_{ji}^\dagger = h_{ij}$ , the global density operator  $\varrho$  evolution

$$\frac{\partial \varrho}{\partial T} = \mathcal{L}_{\text{eff}} \varrho \quad (45)$$

preserves the block-diagonal structure [(33)] of the density operator, i.e.  $\varrho(T) = \sum_i \varrho^{(i)}(T)$ . Therefore, Eq. (45) reduces to

$$\begin{aligned} \frac{\partial}{\partial T} \sum_i \varrho^{(i)} &= -i\gamma \sum_i [h_{ii}, \varrho^{(i)}] \\ &\quad - \frac{\Omega}{2} \sum_{i \neq j} \left( \{h_{ij} h_{ji}, \varrho^{(i)}\} - 2h_{ij} \varrho^{(j)} h_{ji} \right). \end{aligned} \quad (46)$$

Taking into account that  $\sum_{i \neq j} C_j = I - C_i$ , we simplify

$$\begin{aligned} \sum_{i \neq j} \{h_{ij} h_{ji}, \varrho^{(i)}\} &= \{C_i h(I - C_i) h C_i, \varrho^{(i)}\} \\ &= \{(h^2)_{ii} - (h_{ii})^2, \varrho^{(i)}\} \end{aligned} \quad (47)$$

and obtain the Hamiltonian dispersion in each block. The operator  $(h^2)_{ii} - (h_{ii})^2$  does not vanish only if transition terms  $h_{ij}$  are non-zero. Physically, transition terms cause short-period correlations between  $\text{supp} C_j$  and  $\text{supp} C_i$ , which are then destroyed by a measurement. Cancellation of those correlations leads to the decoherence in diagonal blocks  $\varrho^{(i)}$ , and the term  $(h^2)_{ii} - (h_{ii})^2$  quantitatively describes such a decoherence.

Substituting (47) in (46), we obtain

$$\begin{aligned} \frac{\partial}{\partial T} \sum_i \varrho^{(i)} &= -i \sum_i \left( H_i^{\text{eff}} \varrho^{(i)} - \varrho^{(i)} (H_i^{\text{eff}})^\dagger \right) \\ &\quad + \Omega \sum_{i \neq j} h_{ij} \varrho^{(j)} h_{ji}, \end{aligned} \quad (48)$$

where the effective non-Hermitian Hamiltonian reads

$$H_i^{\text{eff}} = \gamma h_{ii} - \frac{i\Omega}{2} \left( (h^2)_{ii} - (h_{ii})^2 \right). \quad (49)$$

The first term in the right-hand side of Eq. (48) can be interpreted as the sum of individual selective evolutions of individual blocks  $\varrho^{(i)}$  in accordance with the results of Sec. II. The second term in the right-hand side of Eq. (48) describes the mutual influence of the blocks.

Note that the maximally mixed state  $\varrho = I/\dim \mathcal{H}_{\text{sys+pr}}$  is a fixed point of the dynamical map (38).

Suppose that all projectors  $C_i$  are one-dimensional, i.e.  $C_i = |i\rangle\langle i|$ , then the density operator (33) is diagonal, with diagonal elements being the probabilities  $p_i(T)$  to observe the outcome  $i$ . According to Eq. (48), the evolution of these probabilities has the form of the classical Pauli equation:

$$\frac{\partial p_i(T)}{\partial T} = \sum_{j \neq i} (W_{j \rightarrow i} p_j(T) - W_{i \rightarrow j} p_i(T)), \quad (50)$$

$$W_{j \rightarrow i} = \Omega |\langle i|h|j\rangle|^2, \quad (51)$$

$$\sum_{j \neq i} W_{i \rightarrow j} = \Omega (\langle i|h^2|i\rangle - \langle i|h|i\rangle^2). \quad (52)$$

Conceptually, Eq. (50) shows that the classical dynamics can be reproduced from the quantum dynamics in the stroboscopic limit of non-selective rank-1 projective measurements of the global system.

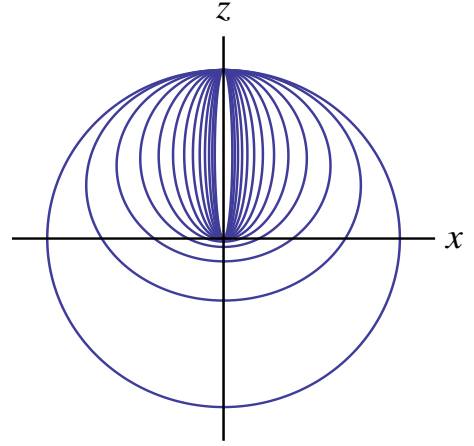


FIG. 6: Evolution of the Bloch ball according to Eq. (59), Example 4, which describes the qubit system evolution when the coupled probe is stroboscopically measured. Parameter  $\Omega = 0.1$ , snapshot interval  $\Delta T = 5$ .

### A. Dynamics of the system and the probe

We now take into account the tensor product structure of the Hilbert space  $\mathcal{H}_{\text{sys+pr}} = \mathcal{H}_{\text{sys}} \otimes \mathcal{H}_{\text{pr}}$ . Non-selective projective measurements of the probe correspond to operators  $C_i = I_{\text{sys}} \otimes P_i$ , where  $P_i = P_i^\dagger = P_i^2$ ,  $\sum_i P_i = I_{\text{pr}}$ , and  $\sum_i \text{rank} P_i = \dim \mathcal{H}_{\text{pr}}$ , see Fig. 5.

Evolution of the system density matrix reads

$$\varrho_{\text{sys}}(T) = \sum_i \text{tr}_{\text{pr}} \varrho^{(i)}(T) \quad (53)$$

and cannot be reduced to the closed formula  $\frac{\partial}{\partial T} \varrho_{\text{sys}} = \mathcal{L}_{\text{sys}} \varrho_{\text{sys}}$  involving  $\varrho_{\text{sys}}$  only, as the partial trace of the semigroup dynamics is not a semigroup dynamics in general. The probe density matrix evolution exhibits the same property.

If  $P_i = |i\rangle_{\text{pr}}\langle i|$  for all  $i$ , then the probe density operator is diagonal  $\varrho_{\text{pr}}(T) = \sum_i p_i(T) |i\rangle_{\text{pr}}\langle i|$  and  $p_i(T) = \text{tr} \varrho^{(i)}(T)$ .

**Example 4.** Consider a two-qubit system, where the first qubit plays the role of a system, and the second qubit is a probe. Let the total Hamiltonian be  $H = \gamma h = \gamma \text{SWAP} = \frac{\gamma}{2} \sum_{j=0}^3 \sigma_j \otimes \sigma_j$ , then  $h^2 = I \otimes I$ . Suppose non-selective projective measurement of the probe qubit in the conventional basis  $|\uparrow\rangle, |\downarrow\rangle$ , then  $C_1 = I \otimes |\uparrow\rangle\langle\uparrow|$  and  $C_2 = I \otimes |\downarrow\rangle\langle\downarrow|$ . A direct calculation yields

$$h_{11} = |\uparrow\rangle\langle\uparrow| \otimes |\uparrow\rangle\langle\uparrow|, \quad (54)$$

$$h_{12} = h_{21}^\dagger = |\downarrow\rangle\langle\uparrow| \otimes |\uparrow\rangle\langle\downarrow|, \quad (55)$$

$$h_{22} = |\downarrow\rangle\langle\downarrow| \otimes |\downarrow\rangle\langle\downarrow|. \quad (56)$$

Substituting Eqs. (54)–(56) in Eq. (48), we get the approximate dynamics of the blocks  $\varrho^{(1)}(T) = \rho^{(1)}(T) \otimes |\uparrow\rangle\langle\uparrow|$  and  $\varrho^{(2)}(T) = \rho^{(2)}(T) \otimes |\downarrow\rangle\langle\downarrow|$  constituting the global

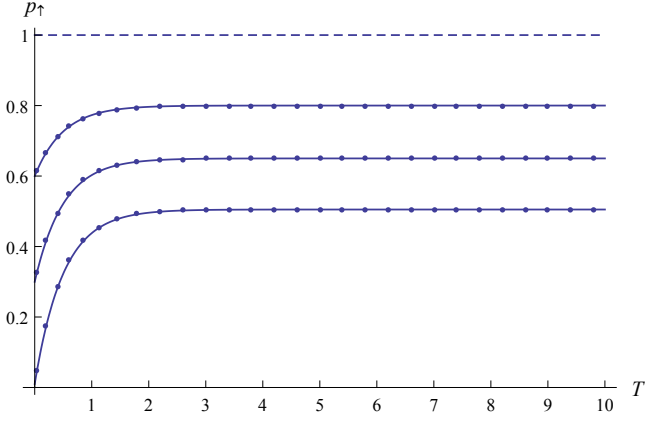


FIG. 7: Comparison of exact (dots) and analytical (solid line) probabilities of finding the qubit system in the excited state at time  $T$  as a result of the stroboscopic evolution (32) and its approximate form (59) with  $\gamma = 5$ ,  $\tau = 0.04$ ,  $\Omega = 1$ , initial state of the system is  $|\psi(0)\rangle = \alpha|\uparrow\rangle + \beta|\downarrow\rangle$ , where  $|\alpha|^2 = 0.01$ ,  $|\beta|^2 = 0.99$  (bottom line),  $|\alpha|^2 = 0.3$ ,  $|\beta|^2 = 0.7$  (middle line), and  $|\alpha|^2 = 0.6$ ,  $|\beta|^2 = 0.4$  (top line). Dashed line corresponds to the evolution with initial state  $|\psi(0)\rangle = |\uparrow\rangle$ .

system+probe density operator  $\varrho(T)$ :

$$\frac{\partial}{\partial T} \begin{pmatrix} \rho_{\uparrow\uparrow}^{(1)} & \rho_{\uparrow\downarrow}^{(1)} \\ \rho_{\downarrow\uparrow}^{(1)} & \rho_{\downarrow\downarrow}^{(1)} \end{pmatrix} = \begin{pmatrix} 0 & (-i\gamma - \Omega/2)\rho_{\uparrow\downarrow}^{(1)} \\ (i\gamma - \Omega/2)\rho_{\downarrow\uparrow}^{(1)} & -\Omega(\rho_{\downarrow\downarrow}^{(1)} - \rho_{\uparrow\uparrow}^{(1)}) \end{pmatrix}, \quad (57)$$

$$\frac{\partial}{\partial T} \begin{pmatrix} \rho_{\uparrow\uparrow}^{(2)} & \rho_{\uparrow\downarrow}^{(2)} \\ \rho_{\downarrow\uparrow}^{(2)} & \rho_{\downarrow\downarrow}^{(2)} \end{pmatrix} = \begin{pmatrix} -\Omega(\rho_{\uparrow\uparrow}^{(2)} - \rho_{\downarrow\downarrow}^{(2)}) & (i\gamma - \Omega/2)\rho_{\uparrow\downarrow}^{(2)} \\ (-i\gamma - \Omega/2)\rho_{\downarrow\uparrow}^{(2)} & 0 \end{pmatrix}. \quad (58)$$

Suppose the initial state of the probe is  $|\uparrow\rangle\langle\uparrow|$  and the initial state of the system is an arbitrary  $2 \times 2$  density matrix  $\varrho_{\text{sys}}(0)$ , then  $\rho^{(1)}(0) = \varrho_{\text{sys}}(0)$  and  $\rho^{(2)}(0) = 0$ . Solving the system of linear equations (57)–(58) and summing  $\varrho_{\text{sys}}(T) = \rho^{(1)}(T) + \rho^{(2)}(T)$ , we get the system density matrix evolution:

$$\varrho_{\text{sys}}(T) = \begin{pmatrix} \varrho_{\text{sys}}^{\uparrow\uparrow}(0) + \frac{1}{2}(1 - e^{-2\Omega T})\varrho_{\text{sys}}^{\downarrow\downarrow}(0) & e^{(-i\gamma - \Omega/2)T}\varrho_{\text{sys}}^{\uparrow\downarrow}(0) \\ e^{(i\gamma - \Omega/2)T}\varrho_{\text{sys}}^{\downarrow\uparrow}(0) & \frac{1}{2}(1 + e^{-2\Omega T})\varrho_{\text{sys}}^{\downarrow\downarrow}(0) \end{pmatrix}. \quad (59)$$

The transformation of the Bloch ball via Eq. (59) is depicted in Fig. 6. One can readily see that the evolution (59) does not have a semigroup property, although the global system-probe dynamics  $\rho^{(1)}(T) \otimes |\uparrow\rangle\langle\uparrow| + \rho^{(2)}(T) \otimes |\downarrow\rangle\langle\downarrow|$  has the semigroup property.

The exact solution of the interrupted evolution (32) is rather involved for the considered example and no concise

closed formula can be obtained. The larger is the number of measurements  $N = \lfloor T/\tau \rfloor$ , the more complicated is the calculation. We compare the approximate analytical solution (59) with the exact numerical solutions in Fig. 7, which shows the agreement between them.

#### IV. CONCLUSIONS

We have considered the quantum system dynamics under frequent successive measurements with a finite repetition rate  $\tau^{-1}$  and derived approximate analytical evolution equations for the timescale  $T \sim (\gamma^2\tau)^{-1}$ , where  $\gamma$  is the characteristic strength of the Hamiltonian.

In the case of selective rank-1 projective measurements of the probe, we have obtained the non-linear system evolution equation for the most probable sequence of coincident outcomes. The pure quantum states remain pure in such an evolution. For selective rank- $r$  projective measurements of the probe, the system evolution becomes more involved and may lead to the change of purity, though the dynamics equation remains non-linear.

In the case of non-selective measurements, the stroboscopic limit  $\gamma^2\tau = \Omega$ ,  $\tau \rightarrow 0$  results in a general Gorini-Kossakowski-Sudarshan-Lindblad equation for the system-probe aggregate, though the reduced evolution of the system may not exhibit the semigroup property. Finally, a classical stochastic Pauli equation is obtained for non-selective projective rank-1 measurements of the system-probe aggregate.

The obtained results can be treated as deviations from the Zeno subspace dynamics, when the interval between measurements  $\tau$  tends to zero and the number of measurements  $N = T/\tau \sim (\gamma\tau)^{-2}$  tends to infinity. The stroboscopic limit provides analytical equations, which can be used in the analysis of experiments with a high but finite repetition rate of repeated measurements at timescale  $T \sim (\gamma^2\tau)^{-1}$ . The examples provided show the agreement between the exact numerical dynamics and the approximate analytical one whenever  $\gamma\tau \ll 1$ .

#### Acknowledgments

The authors thank Luigi Accardi for fruitful discussions. The authors are grateful to the anonymous referee and Pavel Pyshkin for valuable comments. The study in Sec. II was supported by Russian Science Foundation under project No. 16-11-00084 and performed in Moscow Institute of Physics and Technology. The results of section III A were obtained by S.N. Filippov, supported by the Russian Foundation for Basic Research under Project No. 16-37-60070 mol\_a\_dk, and performed at the Institute of Physics and Technology of the Russian Academy of Sciences.

[1] T. Heinosaari and M. Ziman, *The Mathematical Language of Quantum Theory*, Section 5.5.2 (Cambridge University Press, Cambridge, 2012).

[2] A. A. Clerk, M. H. Devoret, S. M. Girvin, F. Marquardt, R. J. Schoelkopf, Introduction to quantum noise, measurement, and amplification, *Rev. Mod. Phys.* **82**, 1155



- (2010).
- [3] F. Buscemi, M. J. W. Hall, M. Ozawa, and M. M. Wilde, Noise and Disturbance in Quantum Measurements: An Information-Theoretic Approach, *Phys. Rev. Lett.* **112**, 050401 (2014).
  - [4] B. Misra and E. C. G. Sudarshan, The Zeno's paradox in quantum theory, *J. Math. Phys.* **18**, 756 (1977).
  - [5] D. Layden, E. Martín-Martínez, and A. Kempf, Perfect Zeno-like effect through imperfect measurements at a finite frequency, *Phys. Rev. A* **91**, 022106 (2015).
  - [6] A. G. Kofman and G. Kurizki, Acceleration of quantum decay processes by frequent observations, *Nature* **405**, 546 (2000).
  - [7] M. C. Fischer, B. Gutiérrez-Medina, and M. G. Raizen, Observation of the Quantum Zeno and Anti-Zeno Effects in an Unstable System, *Phys. Rev. Lett.* **87**, 040402 (2001).
  - [8] P. Facchi, H. Nakazato, and S. Pascazio, From the Quantum Zeno to the Inverse Quantum Zeno Effect, *Phys. Rev. Lett.* **86**, 2699 (2001).
  - [9] T. Kiss, I. Jex, G. Alber, and S. Vymětal, Complex chaos in the conditional dynamics of qubits, *Phys. Rev. A* **74**, 040301(R) (2006).
  - [10] T. Kiss, S. Vymětal, L. D. Tóth, A. Gábris, I. Jex, and G. Alber, Complex chaos in the conditional dynamics of qubits, *Phys. Rev. Lett.* **107**, 100501 (2011).
  - [11] T. Konrad and H. Uys, Maintaining quantum coherence in the presence of noise through state monitoring, *Phys. Rev. A* **85**, 012102 (2012).
  - [12] P. Facchi, D. A. Lidar, and S. Pascazio, Unification of dynamical decoupling and the quantum Zeno effect, *Phys. Rev. A* **69**, 032314 (2004).
  - [13] Y. Li, L.-A. Wu, Y.-D. Wang, and L.-P. Yang, Nondestructive ultrafast ground-state cooling of a mechanical resonator, *Phys. Rev. B* **84**, 094502 (2011).
  - [14] A. Pechen and A. Trushechkin, Measurement-assisted Landau-Zener transitions, *Phys. Rev. A* **91**, 052316 (2015).
  - [15] J. Eisert, M. P. Müller, and C. Gogolin, Quantum measurement occurrence is undecidable, *Phys. Rev. Lett.* **108**, 260501 (2012).
  - [16] T. Heinosaari and T. Miyadera, Universality of sequential quantum measurements, *Phys. Rev. A* **91**, 022110 (2015).
  - [17] A. Di Lorenzo, Sequential Measurement of Conjugate Variables as an Alternative Quantum State Tomography, *Phys. Rev. Lett.* **110**, 010404 (2013).
  - [18] L. Diósi, Structural features of sequential weak measurements, *Phys. Rev. A* **94**, 010103(R) (2016).
  - [19] D. Burgarth, V. Giovannetti, A. N. Kato, and K. Yuasa, Quantum estimation via sequential measurements, *New J. Phys.* **17**, 113055 (2015).
  - [20] H. Bassa, S. K. Goyal, S. K. Choudhary, H. Uys, L. Diósi, and T. Konrad, Process tomography via sequential measurements on a single quantum system, *Phys. Rev. A* **92**, 032102 (2015).
  - [21] R. Raussendorf and H. Briegel, A One-Way Quantum Computer, *Phys. Rev. Lett.* **86**, 5188 (2001).
  - [22] S. Lloyd, V. Giovannetti, and L. Maccone, Sequential Projective Measurements for Channel Decoding, *Phys. Rev. Lett.* **106**, 250501 (2011).
  - [23] Y. Suzuki, M. Iinuma, and H. F. Hofmann, Observation of non-classical correlations in sequential measurements of photon polarization, *New J. Phys.* **18**, 103045 (2016).
  - [24] P. J. Coles and M. Piani, Complementary sequential measurements generate entanglement, *Phys. Rev. A* **89**, 010302(R) (2014).
  - [25] J. Audretsch and M. Mensky, Continuous fuzzy measurement of energy for a two-level system, *Phys. Rev. A* **56**, 44 (1997).
  - [26] A. N. Korotkov, Selective quantum evolution of a qubit state due to continuous measurement, *Phys. Rev. B* **63**, 115403 (2001).
  - [27] J. Audretsch, T. Konrad, and A. Scherer, Sequence of unsharp measurements enabling a real-time visualization of a quantum oscillation, *Phys. Rev. A* **63**, 052102 (2001).
  - [28] J. Audretsch, L. Diósi, and T. Konrad, Evolution of a qubit under the influence of a succession of weak measurements with unitary feedback, *Phys. Rev. A* **66**, 022310 (2002).
  - [29] Q. Ai, D. Xu, S. Yi, A. G. Kofman, C. P. Sun, and F. Nori, Quantum anti-Zeno effect without wave function reduction, *Scientific Reports* **3**, 1752 (2013).
  - [30] C. M. Caves, K. S. Thorne, R. W. P. Drever, V. D. Sandberg, and M. Zimmermann, On the measurement of a weak classical force coupled to a quantum-mechanical oscillator. I. Issues of principle, *Rev. Mod. Phys.* **52**, 341 (1980).
  - [31] V. B. Braginsky and F. Y. Khalili, *Quantum Measurement* (Cambridge University Press, Cambridge, 1992).
  - [32] A. N. Jordan and M. Büttiker, Quantum nondemolition measurement of a kicked qubit, *Phys. Rev. B* **71**, 125333 (2005).
  - [33] R. Ruskov, K. Schwab, and A. N. Korotkov, Squeezing of a nanomechanical resonator by quantum nondemolition measurement and feedback, *Phys. Rev. B* **71**, 235407 (2005).
  - [34] D. Layden, E. Martín-Martínez, and A. Kempf, Universal scheme for indirect quantum control, *Phys. Rev. A* **93**, 040301(R) (2016).
  - [35] M. Ziman and V. Bužek, *Quantum Dynamics and Information (Proc. of 46th Karpacz Winter School of Theoretical Physics)* (World Scientific, Singapore, 2011).
  - [36] T. Rybár, S. N. Filippov, M. Ziman, and V. Bužek, Simulation of indivisible qubit channels in collision models, *J. Phys. B: At. Mol. Opt. Phys.* **45**, 154006 (2012).
  - [37] L. Accardi, Y. G. Lu, and I. Volovich, *Quantum Theory and Its Stochastic Limit* (Springer-Verlag, Berlin, 2002).
  - [38] P. Facchi and S. Pascazio, Quantum Zeno Subspaces, *Phys. Rev. Lett.* **89**, 080401 (2002).
  - [39] Y. Li, D. A. Herrera-Martí, and L. C. Kwek, Quantum Zeno effect of general quantum operations, *Phys. Rev. A* **88**, 042321 (2013).
  - [40] A. G. Kofman, S. Ashhab, F. Nori, Nonperturbative theory of weak pre- and post-selected measurements, *Phys. Rep.* **520**, 43 (2012).
  - [41] M. Navascués and S. Popescu, How energy conservation limits our measurements, *Phys. Rev. Lett.* **112**, 140502 (2014).
  - [42] H.-P. Breuer and F. Petruccione, *The Theory of Open Quantum Systems*, Section 6.1 (Oxford University Press, Oxford, 2002).
  - [43] S. N. Filippov and M. Ziman, Bipartite entanglement-annihilating maps: Necessary and sufficient conditions, *Phys. Rev. A* **88**, 032316 (2013).
  - [44] V. Gorini, A. Kossakowski, and E. C. G. Sudarshan, Completely positive dynamical semigroups of  $N$ -level systems, *J. Math. Phys.* **17**, 821 (1976).
  - [45] G. Lindblad, On the Generators of Quantum Dynamical Semigroups, *Commun. Math. Phys.* **48**, 119 (1976).
  - [46] A. G. Kofman, G. Kurizki, and T. Opatrný, Zeno and anti-Zeno effects for photon polarization dephasing, *Phys. Rev. A* **63**, 042108 (2001).